66. Oligosaccharides Related to Tumor-Associate Antigens

Part 2[1])

Conformational Analysis of the Trisaccharide α-L-Fuc*p*-(1→2)-β-D-Gal*p*-(1→3)-β-D-Gal*p*NAc, Epitope Structure Recognized by the MBr1 Antibody

by **Lucio Toma***

Dipartimento di Chimica Organica, Università di Pavia, Via Taramelli 10, I-27100 Pavia

and **Pierangela Ciuffreda, Diego Colombo,** and **Fiamma Ronchetti**

Dipartimento di Chimica e Biochimica Medica, Università di Milano, Via Saldini 50, I-20133 Milano

and **Luigi Lay** and **Luigi Panza**

Dipartimento di Chimica Organica e Industriale, Università di Milano, Via Venezian 21, I-20133 Milano

(27.XII.93)

The conformational space of the trisaccharide α-L-Fuc-(1→2)-β-D-Gal-(1→3)-β-D-GalNAc-1-OPr (**2**) and of its component disaccharide moieties α-L-Fuc-(1→2)-β-D-Gal-1-OMe (**3**) and β-D-Gal-(1→3)-β-D-GalNAc-1-OPr (**4**) was investigated with the aid of molecular-mechanics energy minimizations and molecular-dynamics simulations. These calculations suggested the occurrence of two conformations for each compound characterized by different ϕ and ψ glycosidic angles. However, ^{1}H-NMR investigation of D_2O solutions of **2–4** indicated a sure preference for one of the two conformers with a contribution of the other one ranging from negligible to low.

Introduction. – The oligosaccharide moieties of glycolipids are involved in a number of biological vital interaction and recognition processes. Glycosphingolipids are normally expressed by human cells, but in the case of cancer cells, aberrant glycosylation and overexpression of some glycosphingolipids are observed [2]. An antigen, isolated from breast-cancer cells, is defined by the monoclonal antibody MBr1; it was demonstrated to have structure **1** [3].

α-L-Fuc-(1→2)-β-D-Gal-(1→3)-β-D-GalNAc-(1→3)-α-D-Gal-(1→4)-β-D-Gal-(1→4)-β-D-Glc-(1→1)-Cer **(1)**

The epitope structure recognized by the antibody was supposed to be the nonreducing terminal trisaccharide due to cross-reactivity of analogous glycolipids sharing the same sequence. Other structures containing the lacto series H structure, α-L-Fuc-(1→2)-β-D-Gal-(1→3)-β-D-GlcNAc, showed no reactivity with the same antibody although they differ only in the orientation of 4-OH of the 2-acetamido-2-deoxy-hexopyranoside residue.

[1]) Part 1: [1].

The three-dimensional structure of the oligosaccharide moiety of glycoproteins and glycolipids is generally considered a significant factor in molecular and cell recognition [4]. Thus, to better characterize the MBr1-defined epitope and to understand the molecular and geometrical basis of its biological function, a project involving the synthesis of fragments of **1**, biological testings, and modeling studies was planned in collaboration with the Istituto Nazionale per lo Studio e la Cura dei Tumori (Milan). After the synthesis [1] of the first of these fragments, the trisaccharide α-L-Fuc-(1→2)-β-D-Gal-(1→3)-β-D-GalNAc-1-OPr (**2**), we decided to get detailed informations on its three-dimensional shape in solution by the use of theoretical methods of conformational analysis combined with high-field ^{1}H-NMR spectroscopy.

Results and Discussion. – Analysis of trisaccharide **2** requires, as a prerequisite, the study of the component disaccharide moieties in order to investigate the conformational properties of the glycosidic linkages as such. So, the theoretical calculations and the spectroscopic investigations were firstly performed on the disaccharides α-L-Fuc-(1→2)-β-D-Gal-1-OMe (**3**) and β-D-Gal-(1→3)-β-D-GalNAc-1-OPr (**4**), and only successively attention was focused on trisaccharide **2**.

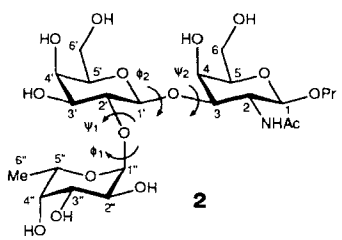

2

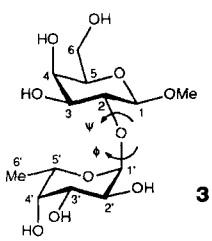

3

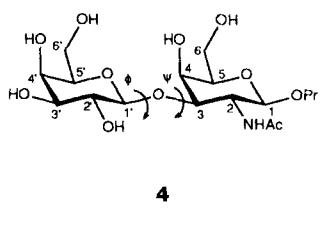

4

The conformational space of disaccharides **3** and **4** was investigated with a molecular-mechanics approach followed by molecular-dynamics simulations. Thirty-six starting geometries were prepared for each disaccharide by rigid rotation around the ϕ and ψ glycosidic bonds covering the entire ϕ/ψ map with a 60° grid. These starting geometries were fully relaxed by using the HyperChem MM$^+$ force field to yield several minima for which the orientations of the CH_2OH and OH groups were optimized. *Table 1* reports the data of the conformers found in a range of 5 kcal/mol above the global minimum of each disaccharide.

Table 1. *Data on the Minimum-Energy Conformations of Disaccharides* **3** *and* **4** *as Calculated by Molecular Mechanics*

	Conformation	ϕ,ψ [°]	E_{rel} [kcal/mol]	Equilibrium percentage
3	**3A**	36, 23	0.47	30.9
	3B	26, −58	0.00	68.3
	3C	21, 173	2.67	0.8
	3D	46, −147	4.75	< 0.1
4	**4A**	39, 20	0.00	75.4
	4B	36, −41	0.74	21.6
	4C	69, 66	1.92	2.9
	4D	169, −5	4.04	0.1

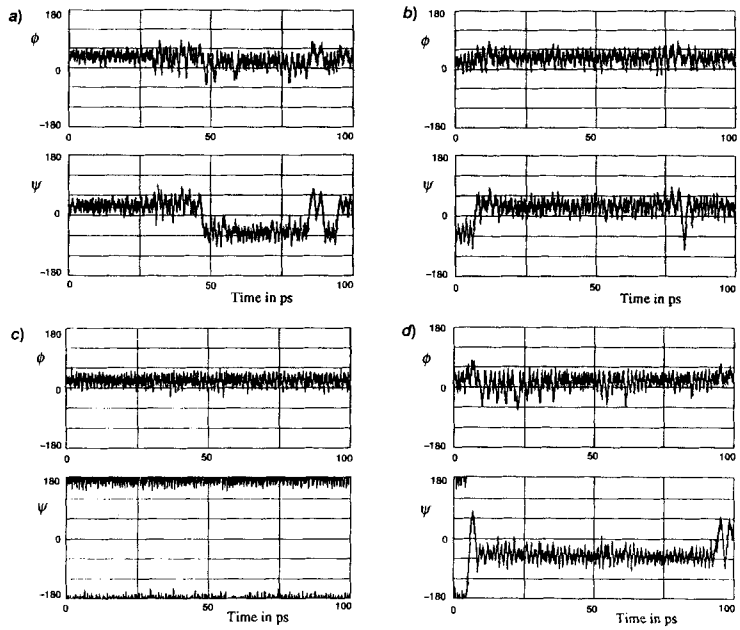

Fig. 1. *History of* ϕ *and* ψ *for the MD simulations starting from* a) **3A**, b) **3B**, c) **3C**, *and* d) **3D** *over the entire trajectory, including equilibration*

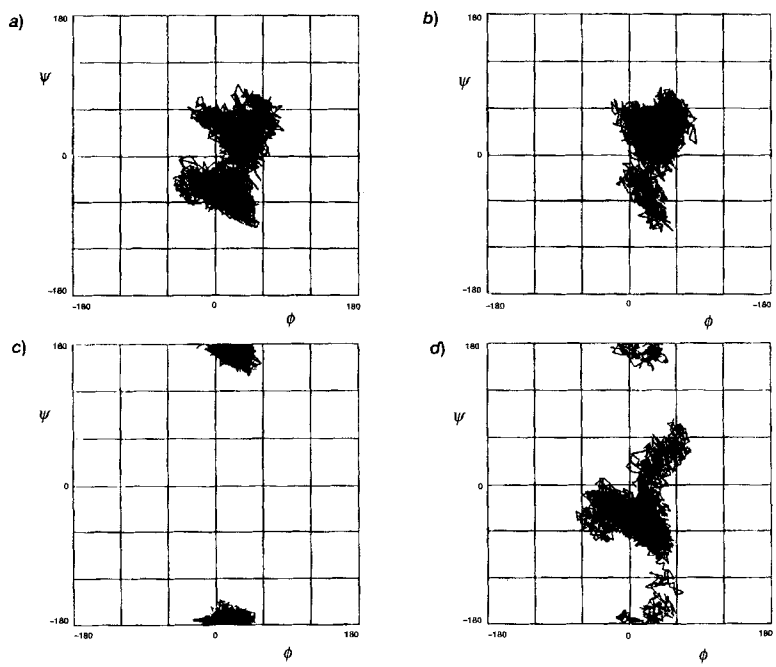

Fig. 2. *Trajectories on the* ϕ/ψ *map for the MD simulations starting from* a) **3A**, b) **3B**, c) **3C**, *and* d) **3D**, *including equilibration*

Both compounds have a minimum – named **A** in the following discussion – located at ϕ values of *ca.* 36–39° and ψ values of *ca.* 20–23° which is the global minimum in the case of **4**. It is accompanied by a second minimum – named **B** – at ϕ *ca.* 26–36°, and ψ *ca.* −41 to −58° which represents the global minimum of **3**. Minima **A** and **B** are practically sufficent to describe the conformational distribution as they account for *ca.* 97–99% of the overall populations.

However, in the modeling of carbohydrates, the large mobility of the OH and CH_2OH groups makes more reliable a dynamic description of the molecules. Molecular-dynamic simulations of compound **3** was thus performed starting from the four minima **3A–D**, consisting in a pre-equilibration period followed by 80-ps data-collection periods. In *Fig. 1* are reported trajectories of the ϕ and ψ angles *vs.* time and in *Fig. 2* the ϕ *vs.* ψ trajectories. Both the simulation starting from **3A** and **3B** showed a few transitions from the **A** region to the **B** one or *vice versa*, easily recognizable in the trajectories of the ψ angle (*Fig. 1*). The two regions are almost equipopulated in a case (*Fig. 2a*), while, in the other case (*Fig. 2b*), the **A** region is largely more populated. No transition was observed in the simulation from **3C**, while a transition to the **A**/**B** region was observed in the simulation from **3D** after *ca.* 5 ps without the occurrence of any back transition. It is interesting to note that in this simulation, the **B** region is more populated than the **A** region.

Analogous simulations were performed for compound **4** (*Figs. 3* and *4*). The energy barrier between the **A** and **B** regions is in this case even lower than for **3**. A higher number of **A** → **B** or **B** → **A** transitions could be observed indicating that minima **4A** and **4B** represent for the disaccharide **4** two conformers of a unique low-energy region. The simulation from **4C** resulted in a transition of the **A**/**B** region after *ca.* 5 ps suggesting that **4C** is not a stable conformation. On the contrary, the simulation from **4D** did not show any transition to more stable regions.

All these results indicate that for the disaccharides **3** and **4**, two conformers (**A** and **B**) seem to be significant for the conformational population of the molecules. The static (*Table 1*) and the dynamic (*Figs. 1–4*) representations predict a large contribute of both of them; however, experimental data are necessary to determine the true balance between conformers **A** and **B**, and ^{1}H-NMR spectroscopy is the most useful tool for such a target. Complete assignment of the ^{1}H-NMR spectrum is a prerequisite to gain insight into the conformations of **3** and **4** in aqueous solution. The ^{1}H-NMR resonances of **3** and **4** were assigned by standard methods that rely on correlation through chemical bonds (COSY, TOCSY, and 2D-NOE experiments) and are reported in *Table 2*, while *Table 3* reports the inter-residue contacts obtained from the phase-sensitive NOESY experiment together to the derived H–H distances referenced to an inter-residue distance used for calibration. Moreover, in *Table 3* are reported the corresponding distances either calculated for the different energy minima of compounds **3** and **4** or averaged from the MD simulations as $r = [< r^{-3} >]^{-1/3}$ [5], taking into account the nonlinear distance dependence of the NOE.

Several inter-residue contacts could be detected for disaccharide **3**; in fact, besides the high interactions H–C(1′)/H–C(2) and H–C(1)/MeO, the interactions of H–C(1′) with H–C(1) and H–C(3), of MeO with H–C(5′) and Me(6′) and of H–C(5′) with H–C(1) and H–C(2) could be detected. The calculated distances closely resemble the distances found for conformer **3A**. The MD simulation starting from **3B** is also in quite a good agreement with such a result: the averaged distances are very close to those obtained from NOESY. It is worthy pointing out that during this MD simulation, the molecule spends

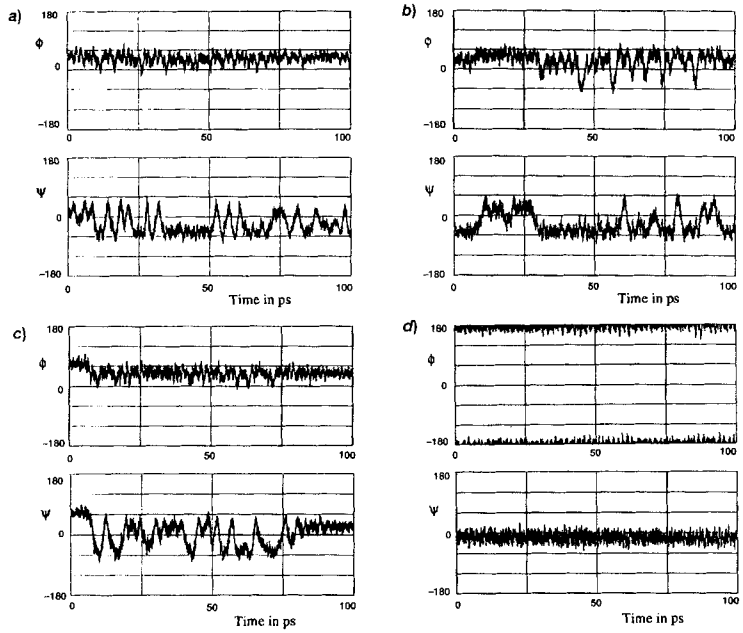

Fig. 3. *History of* ϕ *and* ψ *for the MD simulations starting from* a) **4A**, b) **4B**, c) **4C**, *and* d) **4D** *over the entire trajectory, including equilibration*

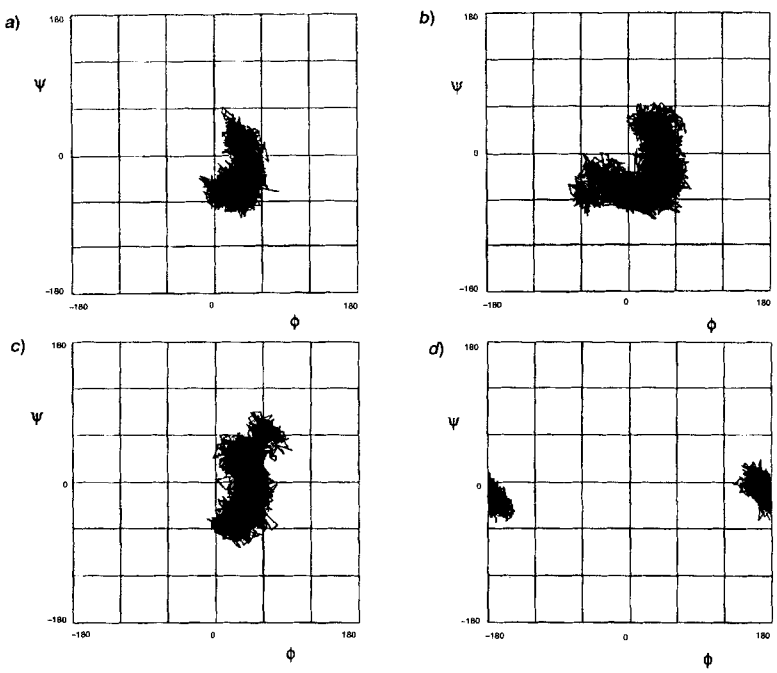

Fig. 4. *Trajectories on the* ϕ/ψ *map for the MD simulations starting from* a) **4A**, b) **4B**, c) **4C**, *and* d) **4D**, *including equilibration*

Table 2. *^{1}H-NMR Spectral Data* (D_2O, 500 MHz) *for Compounds* **2**–**4**. δ(H) Values in ppm referenced to HDO at 4.55 ppm, J in Hz; n.d. = not determined.

Disaccharide **3**			Disaccharide **4**			Trisaccharide **2**		
	δ	J		δ	J		δ	J
H–C(1′)	4.94	$J(1',2')$ = 4.3				H–C(1″)	5.05	$J(1'',2'')$ = 4.3
H–C(2′)	3.60	$J(2',3')$ = 10.0				H–C(2″)	3.59	$J(2'',3'')$ = 10.8
H–C(3′)	3.68	$J(3',4')$ = 3.6				H–C(3″)	3.47	$J(3'',4'')$ = 3.6
H–C(4′)	3.63	$J(4',5')$ < 1				H–C(4″)	3.55	$J(4'',5'')$ < 1
H–C(5′)	4.07	$J(5',6')$ = 6.5				H–C(5″)	4.06	$J(5'',6'')$ = 6.5
Me(6′)	1.03					Me(6″)	1.03	
H–C(1)	4.23	$J(1,2)$ = 7.9	H–C(1′)	4.26	$J(1',2')$ = 7.9	H–C(1′)	4.42	$J(1',2')$ = 7.5
H–C(2)	3.34	$J(2,3)$ = 9.5	H–C(2′)	3.35	$J(2',3')$ = 10.8	H–C(2′)	3.46	$J(2',3')$ = 10.0
H–C(3)	3.65	$J(3,4)$ = 3.6	H–C(3′)	3.44	$J(3',4')$ = 3.5	H–C(3′)	3.65	$J(3',4')$ = 3.6
H–C(4)	3.73	$J(4,5)$ < 1	H–C(4′)	3.73	$J(4',5')$ < 1	H–C(4′)	3.71	$J(4',5')$ < 1
H–C(5)	3.50	$J(5,6a)$ = 7.9	H–C(5′)	3.47	$J(5',6'a)$ = 7.9	H–C(5′)	3.47	$J(5',6'a)$ n.d.
H_a–C(6)	3.62	$J(5,6b)$ = 4.3	H_a–C(6′)	3.59	$J(5',6'b)$ = 4.3	H_a–C(6′)	3.56–3.63	$J(5',6'b)$ n.d.
H_b–C(6)	3.57	$J(6a,6b)$ = 11.5	H_b–C(6′)	3.55	$J(6'a,6'b)$ = 11.5	H_b–C(6′)	3.56–3.63	$J(6'a,6'b)$ n.d.
			H–C(1)	4.33	$J(1,2)$ = 8.5	H–C(1)	4.14	$J(1,2)$ = 7.9
			H–C(2)	3.81	$J(2,3)$ = 10.8	H–C(2)	3.80	$J(2,3)$ = 10.8
			H–C(3)	3.69	$J(3,4)$ = 3.2	H–C(3)	3.74	$J(3,4)$ = 2.9
			H–C(4)	3.99	$J(4,5)$ < 1	H–C(4)	3.92	$J(4,5)$ < 1
			H–C(5)	3.51	$J(5,6a)$ = 7.9	H–C(5)	3.52	$J(5,6a)$ = 7.9
			H_a–C(6)	3.62	$J(5,6b)$ = 4.3	H_a–C(6)	3.56–3.63	$J(5,6b)$ = 4.3
			H_b–C(6)	3.57	$J(6a,6b)$ = 11.5	H_b–C(6)	3.56–3.63	$J(6a,6b)$ n.d.
MeO	3.40		CH_aO	3.39	$J(H_a,H_b)$ = 10.0	CH_aO	3.31	$J(H_a,H_b)$ 10.0
			CH_bO	3.67	$J(H_a,CH_2)$ = 7.2	CH_bO	3.67	$J(H_a,CH_2)$ 6.5
			CH_2	1.38	$J(H_b,CH_2)$ = 7.2	CH_2	1.35	$J(H_b,CH_2)$ 6.0
			Me	0.69	$J(CH_2,Me)$ = 7.2	Me	0.68	$J(CH_2,Me)$ 7.6
			Ac	1.84		Ac	1.85	

most of the time in the **A** region, while, in the simulation from **3A**, the two **A** and **B** regions are almost equally populated.

Disaccharide **4** showed a much smaller number of inter-residue contacts. Besides the high interaction H–C(1′)/H–C(3), only two low interactions of H–C(1′) with H–C(2) and H–C(4) were detected. A comparison of the NOE distances with those calculated for conformers **4A–D** indicates that **4A** shows the best agreement between the experimental and calculated values; conformer **4B** should have given rise to a much higher H–C(1′)/H–C(4) volume. The MD simulations predict similar populations for the **A** and **B** conformers, contrary to the results of the NMR data which indicate a preference for the **A** region. In conclusion, also in this case, the molecule spends most of the time in the region of conformer **4A**.

The exploration of the conformational space of trisaccharide **2** through molecular-mechanics optimizations was limited to the regions allowed for the component disaccharides: so, we chose as starting geometries of **2** all the conformations showing glycosidic-bond dihedral angles corresponding to the values found as minima for the component disaccharides. After minimization and optimization of the orientation of the CH_2OH and OH groups, seven minima were found in a range of 5 kcal/mol above the global minimum. *Table 4* reports the data of these minima and *Fig. 5* shows the 3D plots

Table 3. *Inter-Residue Contacts Derived from the Phase-Sensitive NOESY Experiments and Corresponding Distances from MM and MD Calculations*

	NOESY Cross-peak volume	Calc. distance [Å] (from NOESY)	Calc. distance for [Å] the minimum-energy conformation				Calc. distance [Å] in the MD simulation	
			3A	**3B**	**3C**	**3D**	from **3A**	from **3B**
H–C(1)/H–C(3)[a])	1	2.70	2.69	2.75	2.83	2.76	2.73	2.71
H–C(1′)/H–C(1)	0.071	4.20	4.53	3.60	2.18	2.21	3.91	4.46
H–C(1′)/H–C(2)	2.359	2.34	2.31	2.31	3.59	3.42	2.34	2.38
H–C(1′)/H–C(3)	0.228	3.45	3.66	4.45	2.31	3.65	3.78	3.47
H–C(5′)/H–C(1)	0.242	3.42	3.42	2.78	5.09	4.25	3.24	3.54
H–C(5′)/H–C(2)	0.201	3.53	3.46	4.28	3.59	3.99	3.66	3.34
H–C(5′)/MeO	0.428	3.33	3.40	4.53	6.80	6.59	4.03	3.57
Me(6′)/MeO	0.305	3.95	4.34	3.82	8.81	7.40	4.43	4.67
H–C(1)/MeO	1.314	2.76	2.73	2.75	2.74	2.74	2.74	2.74
	NOESY Cross-peak volume	Calc. distance [Å] (from NOESY)	Calc. distance for [Å] the minimum-energy conformation				Calc. distance [Å] in the MD simulation	
			4A	**4B**	**4C**	**4D**	from **4A**	from **4B**
H–C(1)/H–C(5)[a])	1	2.40	2.40	2.40	2.37	2.42	2.40	2.39
H–C(1′)/H–C(2)	0.087	3.61	3.77	4.49	2.74	4.47	4.29	4.19
H–C(1′)/H–C(3)	0.987	2.40	2.33	2.27	3.26	3.52	2.25	2.30
H–C(1′)/H–C(4)	0.073	3.71	4.22	2.61	4.62	4.25	3.15	2.84
	NOESY Cross-peak volume	Calc. distance [Å] (from NOESY)[b])	Calc. distance for [Å] the minimum-energy conformation				Calc. distance [Å] in the MD simulation	
			2AA	**2BB**			from **2AA**	from **2BB**
H–C(1′)/H–C(3′)[a])	1	2.65	2.66	2.72			2.67	2.72
H–C(1″)/H–C(2′)	2.340	2.30	2.36	2.27			2.42	2.27
H–C(5″)/H–C(1′)	0.151	3.63	3.52	2.92			3.66	3.10
H–C(5″)/H–C(2)	1.045	2.63	2.43	6.01			2.73	6.19
Me(6″)/H–C(2)	0.307	3.45	3.62	5.53			3.76	5.83
H–C(1′)/H–C(3)	1.947	2.37	2.42	2.26			2.40	2.28
H–C(3″)/Ac	0.581	3.10	3.14	5.75			3.41	6.11

[a]) Intra-residue contact used for calibration.
[b]) These values are in close agreement with those calculated from the ROESY experiments.

Table 4. *Data on the Minimum-Energy Conformations of Trisaccharide* **2** *as Calculated by Molecular Mechanics*

Conformation	ϕ_1,ψ_1 [°]	ϕ_2,ψ_2 [°]	E_{rel} [kcal/mol]	Equilibrium percentage
2BB	22, −54	29, −53	0.00	75.5
2AA	36, 27	40, 27	0.71	22.8
2BC	23, −54	67, 70	2.66	0.9
2CA	22, 174	55, 52	3.05	0.4
2AC	32, 29	68, 66	3.21	0.3
2CB	22, 173	23, −54	4.25	< 0.1
2AB	40, 38	32, −57	4.36	< 0.1

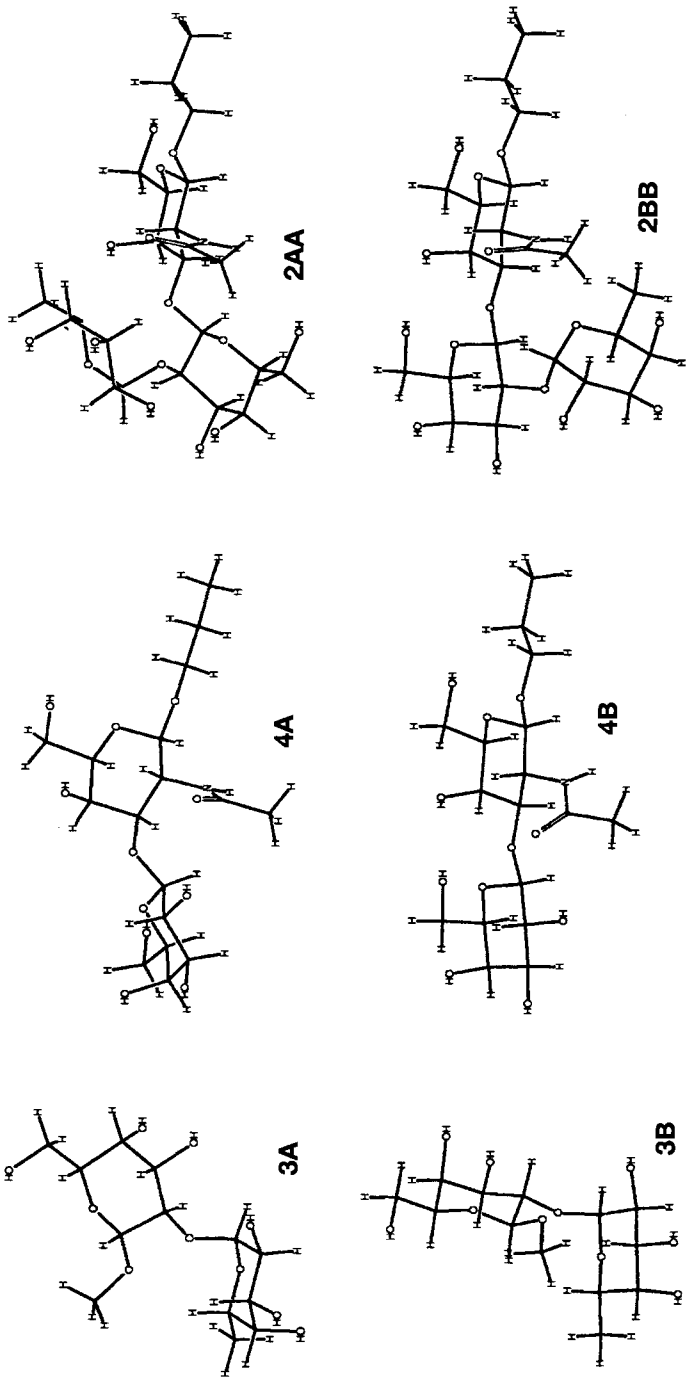

Fig. 5. *Three-dimensional plots of the most populated conformers of disaccharides* **3** *and* **4** *and trisaccharide* **2**

of the most populated conformers. The results indicate that the conformation of one glycosidic linkage heavily influences the conformation of the other one. In fact, a conformation of type **A** at the first linkage requires a conformation of the same type at the second one, while **B** requires **B**: confomers **2AA** and **2BB** are the two lowest-energy minima and are indicated by the calculations as the two only populated conformations of the molecule.

Once again, two MD simulations were performed on the trisaccharide **2** starting from the conformers **2AA** and **2BB**. In *Figs. 6* and *7* are reported the ϕ and ψ trajectories. Contrary to compounds **3** and **4**, no conformational transition was observed during the simulation neither from the **2AA** to the **2BB** conformation nor *vice versa*. This more rigid behaviour could be explained by the consideration that such a transition would require a cooperative movement at both the glycosidic linkages (with a coordinate movement around four single bonds) or the intermediacy of a high-energy conformer like **2AB**.

Also in the case of **2** the 2D-NOE experiments allowed to quantify the contribution of each of the two conformers to the overall population. In addition to the expected intra-residue and inter-residue contacts, some short contacts between the fucose and the *N*-acetyl-galactosamine residue were observed in the NMR experiment; in particular, a very high H–C(5″)/H–C(2) interaction accompanied by the not negligible Me(6″)/H–C(2) and H–C(3″)/Ac interactions. These contacts surely indicate **2AA** as the populated conformer. Inspection of the inter-residue distances predicted by the MD simulation starting from this conformer and the corresponding NOESY-calculated ones indicates a close agreement of the two series of values (*Table 3*).

It can be concluded that while the molecular-mechanics optimizations and the molecular-dynamics simulations suggest the occurrence of two conformations for compound **2**, the 2D-NOE data can be explained by the conformer **2AA** alone. Other trisaccharides, sharing with **2** the same fucosylgalactosyl moiety but differing in the third residue, were investigated [6–8] both by theoretical and NMR approaches. α-L-Fuc-(1→2)-β-D-Gal-(1→3)-β-D-GlcNAc-OMe was shown by *Bush* and coworkers [6] to have a conformation similar to **2AA** (ϕ_1 and ψ_1 50 and 10°, resp.; ϕ_2 and ψ_2 40 and 10°, resp.) indicating that the orientation of 4-OH of the third residue has no significant influence on the conformation of trisaccharide **2**. Also in the case of α-L-Fuc-(1→2)-β-D-Gal-(1→4)-β-D-GlcNAc-OMe [7], only one conformer was obtained having the fucosylgalactose linkage in the **A**-type conformation (ϕ_1 and ψ_1 49 and 21°, resp.); on the contrary, in the case of α-L-Fuc-(1→2)-β-D-Gal-(1→4)-D-Glc [8], two regions of the ϕ/ψ space appeared populated, the first corresponding to the **A** region and the second close to the **B** one. Our calculations indicate a high conformational mobility around the glycosidic linkages in disaccharide **4** though this mobility is strongly lowered in trisaccharide **2**; no transition between conformers **2AA** and **2BB** could be observed in the MD simulations, indicating a relatively high energy barrier between them. Though the NMR data indicate **2AA** as the only populated conformer in solution, conformation **2BB** should be relatively easily accessible, and it cannot be excluded as relevant conformer in the interaction with the receptor.

We gratefully acknowledge financial support provided by the Italian *Ministero dell'Università e della Ricerca Scientifica e Tecnologica*, Roma, and *Consiglio Nazionale delle Ricerche*, Roma. We also express our thanks to Prof. *Giovanni Russo* for helpful discussions.

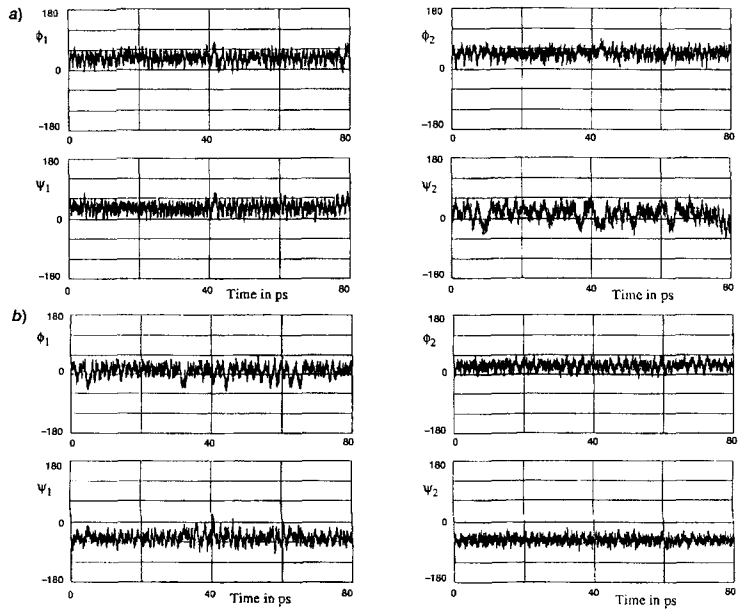

Fig. 6. *History of* ϕ_1, ψ_1, *and* ϕ_2, *and* ψ_2 *for the MD simulations starting from* a) **2AA** *and* b) **2BB** *over the data-collection period*

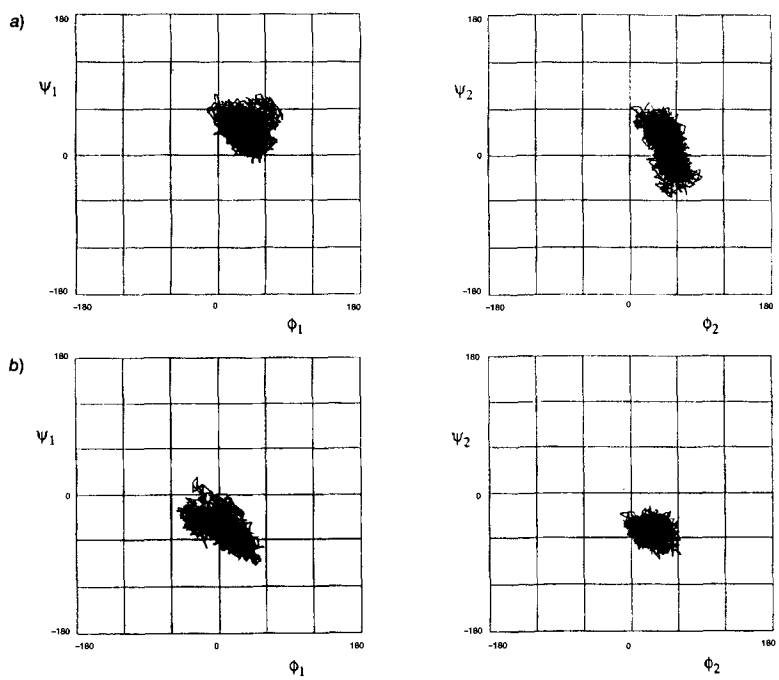

Fig. 7. *Trajectories on the* ϕ_1/ψ_1 *and* ϕ_2/ψ_2 *maps for the MD simulations starting from* a) **2AA** *and* b) **2BB** *over the data-collection period*

Experimental Part

Compounds **2**–**4**. The synthesis of propyl 2-acetamido-2-deoxy-3-*O*-[2-*O*-(α-L-fucopyranosyl)-β-D-galactopyranosyl]-β-D-galactopyranoside (**2**) was described in [1]. Methyl 2-*O*-(α-L-fucopyranosyl)-β-D-galactopyranoside (**3**) was obtained from 1,3,4,6-tetra-*O*-acetyl-2-*O*-(2,3,4-tri-*O*-benzyl-α-L-fucopyranosyl)-α-D-galactopyranose [9] through methylation of the anomeric position of galactose *via* the trichloroacetimidate route and removal of the protecting groups [10]: oil, $[\alpha]_{20}^{D} = -87.5$ ($c = 1$, MeOH). Propyl 2-acetamido-2-deoxy-3-*O*-(β-D-galactopyranosyl)-β-D-galactopyranoside (**4**) was obtained from allyl 2-acetamido-3-*O*-(2-*O*-acetyl-3,4,6-tri-*O*-benzyl-β-D-galactopyranosyl)-2-deoxy-4,6-di-*O*-pivaloyl-β-D-galactopyranoside [1] through deacylation (0.01N MeONa, MeOH) and hydrogenolysis (H_2, Pd/C, MeOH): oil, $[\alpha]_{20}^{D} = -4.1$ ($c = 1$, MeOH).

^{1}H-NMR Experiments. Compounds **2**–**4** were exchanged and lyophilized twice in 99.8% D_2O (*Merck*) and dried under high vacuum before dissolving in 99.96% D_2O (*Aldrich*) under N_2 (0.05M solns.). ^{1}H-NMR Spectra: at 303 K; *Bruker-AM500* spectrometer equipped with an *Aspect-3000* computer, a process controller, and an array processor; assignments by a combination of 1D and 2D COSY [11], TOCSY [12], NOESY [13], and ROESY [14] experiments. TOCSY Spectra: MLEV-17 phase scheme [12], total mixing time 180 ms; 512 TPPI experiments, 32 transients per t_1, relaxation delay 1.5 s; data were transformed as 2 K × 1 K matrix. NOESY Spectra: TPPI mode using the pulse sequence described in [13]; 512 t_1 increments (32 scans for each), spectral size in the time domain 2 K and spectral width 3030 Hz; zero filling to 1 K in the t_1 dimension before *Fourier* transformation; the linearity in the build up of the NOE intensity was tested by performing the experiments at different mixing times (350–800 ms), and no significant differences were found in the calculated distance obtained from the different data set. ROESY Spectra: phase-sensitive mode, pulse sequence 90-t_1-SL-FID where SL stands for a continuous spin-lock pulse of 200 ms at a field strength corresponding to a 90-deg pulse width between 100–125 μs. All 2D spectra were weighted with the squared sine-bell function shifted by $\pi/2$ in both dimensions. H–H Distances were calculated from equation $r_i = r_j (V_i/V_j)^{-1/6}$ where V_i and V_j are the cross-peak volumes from unknown and calibration distances (r_i, r_j), respectively, measured by standard *Bruker* 2D integration routine from 2D-NOESY and 2D-ROESY spectra. The cross-peak volumes for the interactions H/Me and Me/Me were divided by 1.5 and 3, resp., before the application of the above equation according to *Macura* and *Ernst* [15] who showed that the NOESY cross-peak intensity is proportional to $N_iN_j/(N_i + N_j)$ where N_i and N_j are the number of i and j protons.

MM and MD Calculations. Molecular-mechanics energy minimizations and molecular-dynamics simulations were performed with the *Autodesk* HyperChem software. The MD simulations started from the optimized structures obtained by minimizations; the molecules were allowed to equilibrate at 300 K for 20 ps followed by a 80-ps period of data collection. A time step of 1 fs was used in the integration algorithm, and the trajectories were saved every 10 fs for further analysis. The H–H distances reported in *Table 3* were averaged over the period of data collection as $r = [< r^{-3} >]^{-1/3}$ [5] as used for fast conformational changes. The glycosidic angles ϕ and ψ were defined by H–C(1′)–O–C(x) and C(1′)–O–C(x)–H, respectively ($x = 2$ for **3**, $x = 3$ for **4**). The glycosidic angles of compound **2** were defined as ϕ_1 H–C(1″)–O–C(2′), ψ_1 C(1″)–O–C(2′)–H, ϕ_2 H–C(1′)–O–C(3), and ψ_2 C(1′)–O–C(3)–H.

REFERENCES

[1] L. Lay, F. Nicotra, L. Panza, G. Russo, E. Adobati, *Helv. Chim. Acta* **1994,** *77,* 509.
[2] S. Hakomori, *Cancer Cells* **1991,** *3,* 461.
[3] E.G. Bremer, S.B. Levery, S. Sonnino, R. Ghidoni, S. Canevari, R. Kannagi, S. Hakomori, *J. Biol. Chem.* **1984,** *259,* 14773.
[4] K. Bock, *Pure Appl. Chem.* **1987,** *59,* 1447; K.-A. Karlsson, *ibid.* **1987,** *59,* 1477.
[5] J. Tropp, *J. Chem. Phys.* **1980,** *72,* 6035.
[6] P. Cagas, K. Kaluarachchi, C.A. Bush, *J. Am. Chem. Soc.* **1991,** *113,* 6815.
[7] C. Mukhopadhyay, C.A. Bush, *Biopolymers* **1991,** *31,* 1737.
[8] A. Ejchart, J. Dabrowsky, C.-W. v.d. Lieth, *Magn. Reson. Chem.* **1992,** *30,* S105.
[9] F. Nicotra, L. Panza, A. Romanò, G. Russo, *J. Carbohydr. Chem.* **1992,** *11,* 397.
[10] L. Panza, unpublished results.
[11] K. Nagayama, A. Kumar, K. Wuetrich, R.R. Ernst, *J. Magn. Reson.* **1980,** *40,* 321.
[12] A. Bax, D.G. Davis, *J. Magn. Reson.* **1985,** *65,* 355.
[13] G. Bodenhausen, H. Kogler, R.R. Ernst, *J. Magn. Reson.* **1984,** *58,* 370.
[14] A. Bax, D.G. Davis, *J. Magn. Reson.* **1985,** *63,* 207.
[15] S. Macura, R.R. Ernst, *Mol. Phys.* **1980,** *41,* 95.